Journal of The Electrochemical Society, **148** (4) A368-A373 (2001)
0013-4651/2001/148(4)/A368/6/$7.00 © The Electrochemical Society, Inc.

Characterization of High Porosity Carbon Electrodes Derived from Mesophase Pitch for Electric Double-Layer Capacitors

To-Chi Weng and Hsisheng Teng[z]

Department of Chemical Engineering, National Cheng Kung University, Tainan 70101, Taiwan

High porosity carbons prepared from mesophase pitch with KOH etching to different extents were used to fabricate electrodes for electric double-layer capacitors. Nitrogen adsorption was used to characterize the porous structure of the carbon electrodes. The performance of the capacitors in 1 M H_2SO_4 was investigated with voltage sweep cyclic voltammetry and constant current charge-discharge cycling. These two electrochemical methods gave fairly close results for capacitance measurements and demonstrated that distributed capacitance along a micropore path affected the capacitor performance. The specific capacitance of the electrodes was found to increase with the specific surface area. However, the capacitance per unit carbon area showed a decreasing trend with the specific area, and this has been attributed to the increased electrode resistance that would probably result from the deepening of the pores upon etching. The highest specific capacitance of 130 F g^{-1} was achieved with an electrode consisting of 80% carbon powders with a specific surface area of 2860 m^2 g^{-1} and 20% polyvinylidenefluoride as the binder.
 [DOI: 10.1149/1.1357171]

Manuscript submitted July 5, 2000; revised manuscript received October 30, 2000.

The electric double-layer capacitor (EDLC) has recently drawn considerable attention as an intermediate power source between rechargeable batteries and conventional capacitors.[1] Rechargeable batteries are generally fabricated to have a large amount of energy storage with relatively low power density, while capacitors can generally supply high specific powers, but their energy capacities are usually low. In an EDLC, the double layer at the electrode/electrolyte interface can be quickly formed, resulting in a high power rate of the EDLC compared to a battery where mass transfer over long distances is required.[2] On the basis of the mechanism for double-layer formation, it is generally true that the larger surface area that an EDLC can provide for adsorption of electrolytes on electrodes, the more energy can be stored in the EDLC.[2-6]

Activated carbons with large surface area and porosity are suitable candidates as materials for the polarizable electrodes in EDLC.[1-13] Almost any carbonaceous material can be converted into activated carbon.[14] The porosity in the carbons can be created by heat-treatment of the carbon precursors combined with etching, which results in carbonization as well as porosity development. Practically, the type of porosity is dictated by the type of precursor material employed; however, the method of preparation is another parameter which may influence the final pore size distribution.[15,16] Mesophase pitch, which is composed of lamellar macromolecules in parallel stack and has a dense structure, may have the potential application in producing high specific capacity electrodes for EDLC. The present study has used mesophase pitch as the precursor of the activated carbon for EDLC electrodes.

The creation of porosity in the carbon derived from mesophase pitch is achieved by etching with potassium hydroxide in the present work. The key mechanisms in porosity development are associated with carbon gasification by the emitted CO_2 and the oxygen contained in the alkali.[17,18] During heat-treatment of the pitch impregnated with KOH, the release of CO_2 from K_2CO_3 formed in the treatment becomes significant at high temperatures. The released CO_2 can react with carbon atoms to open up closed pores and enlarge existing micropores. Meanwhile, the potassium-containing compounds, such as K_2O and K_2CO_3, can be reduced by carbon to form K metal, thus causing the carbon gasification and hence the formation of pores. The etching process can also be conducted with physical methods, gasification of a char as in oxidizing gases, such as CO_2 or steam.[19] Carbon etching with KOH has been reported to be more effective in porosity development than those with physical methods.[16,18]

Changes in porous structures during etching are often monitored and controlled to produce various porous carbons for different applications. The purpose of this work is to investigate the applicability of using carbons derived from mesophase pitch as an electrode material. An effort is also devoted to the effects of the porous structure, which are characterized with N_2 adsorption, on the electrochemical behavior and capacitance of the resulting electrodes for EDLCs.

Experimental

Sample preparation.—The precursor of the porous carbons used in the EDLC was a mesophase pitch powder generated by heat-treatment of a coal-tar pitch having 3-6% primary QI (quinoline insolubles) with a softening point of 85-90°C. The anisotropic mesophase powder was obtained by extracting the heat-treated pitch with a suitable solvent. The characteristics of the precursor coal-tar pitch and the mesophase powder are listed in Table I. Prior to any further treatment the mesophase powder was ground and sieved to have an average size of 20 μm.

Porous carbons were prepared from the heat-treatment of the pitch impregnated with KOH. In a 250 mL glass-stoppered flask, the KOH-impregnation process was initiated by mixing 1 g of the mesophase powder with a KOH solution containing 60 g of water. The flask was immersed in a constant-temperature shaker bath, with a shaker speed of 100 rpm. The mixing was performed at 85°C and lasted for 3 h. The concentration of the KOH solution was adjusted to give a ratio of KOH to pitch (*i.e.*, a chemical ratio) varying in a range one to five by weight.

After mixing, the pitch-KOH slurry was subjected to vacuum drying at 110°C for 24 h. The dried samples were then heat-treated in a horizontal cylindrical furnace (60 mm id) under an N_2 flow at 100 mL/min. The treatments were initiated by heating the sample at 2.5°C/min from room temperature to 700°C, followed by holding the sample at the temperature for 1 h before cooling under N_2.

After cooling the etched products were washed by stirring with 250 mL of an HCl solution of 0.5 N in concentration at 85°C for 30 min, followed by filtration. The acid-washed sample was then leached by mixing with 250 mL of distilled water at 85°C, followed by filtration of the mixtures. Leaching was carried out several times until the pH value of the water-carbon mixture was above 6. The leached products were then dried in vacuum at 110°C for 24 h, to give the porous carbon products.

Carbon characterization.—Specific surface areas and pore volumes of the derived carbons were determined by gas adsorption. An automated adsorption apparatus (Micromeritics, ASAP 2010) was

[z] E-mail: hteng@mail.ncku.edu.tw

Table I. Characteristics of precursor coal-tar pitch and mesophase pitch powder.

Characteristics	Precursor coal-tar pitch	Mesophase pitch powder
Softening point (°C)	85-90	
Quinoline insolubles (%)	3-6	85-99
Toluene insolubles (%)	25-30	95-99
Fixed carbon (%)	40-46	86-92
Heat-treatment extraction yield (%)		35-45
Ash (%)		0.1-0.4

employed for these measurements. Adsorption of N_2 was performed at −196°C. Nitrogen surface areas and micropore volumes of the samples were determined from the Brunauer-Emmett-Teller (BET) and Dubinin-Radushkevich (D-R) equations, respectively. The amount of N_2 adsorbed at relative pressures near unity ($p/p_0 = 0.98$ in this work) has been employed to determine the total pore volume, which corresponds to the sum of the micropore and mesopore volumes.[20] The average pore diameter can be estimated according to the surface area and total pore volume, if the pores are assumed to be parallel and cylindrical.

Preparation of electrodes.—Carbons with different porosities, produced by adjusting the KOH/pitch ratio during etching, were used to fabricate electrodes. Prior to the formation of electrodes for electrochemical tests, each carbon was added to a solution of polyvinylidenefluoride (PVDF) in *N*-methyl pyrrolidinone (NMP), and the mixture was mixed at ambient temperature to form a carbon slurry. Electrodes were prepared by pressing the slurry on stainless steel foils with a doctor blade, followed by evaporating the solvent, NMP, with a blow dryer. The carbon layer, which consisted of 20 wt % PVDF as the binding material, was adjusted to have a thickness of 150 μm.

Electrochemical measurements.—A sandwich-type cell was prepared with a pair of the carbon electrodes and a piece of filter paper as the separator. In electrochemical measurements the electrolyte was a 1 M H_2SO_4 aqueous solution. Cyclic voltammetric measurements of the cell were made in the potential range of −0.9 to 0.9 V applied between the two electrodes. The rate of the potential scan ranged from 2 to 10 mV s^{-1}. The capacitance of the cells was measured by charging the capacitors to a voltage of 0.9 V and then discharging to 0 V at a constant current. All the electrochemical measurements were conducted at ambient temperature.

Results and Discussion

Characteristics of the porous carbons for electrodes.—The porous structures of the carbons derived from the mesophase pitch are presented in Table II. The carbons with different porosities were prepared by varying the KOH/pitch ratio within one to five during etching. The porosity of the carbons increases with the increasing ratio, indicating that the etching intensity has been enhanced with the increased addition of the alkali. In the table each carbon has been designated by using the nomenclature of its precursor, mesophase pitch (MP), followed by one-tenth of its BET surface area. The pore size distribution shows that with the increase in surface area the mesopore fraction decreases to reach a minimum and then increases with a further increase of the porosity. The decrease in mesopore fraction indicates that by increasing the KOH/pitch ratio more KOH molecules can diffuse into the interior of the pitch to create microporosity. With further increase in KOH impregnation, the existing micropores were then widened by extensive gasification, hence resulting in the increase in mesopore fraction.

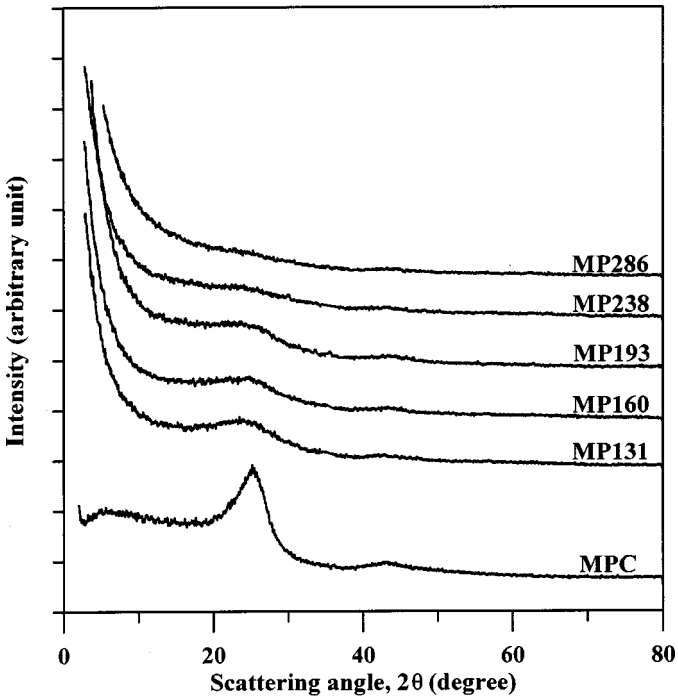

Figure 1. Powder X-ray diffraction patterns of the carbons derived from KOH etching of mesophase pitch to different extents.

As for the crystalline structure, the X-ray diffraction (XRD) patterns of the carbons with different porosities are shown in Fig. 1. The carbon derived from the 700°C treatment of the pitch without KOH impregnation, which is designated as MPC in the figure, is also characterized with XRD for comparison. The crystallites in carbon have a scattering angle (2θ) near 23° in XRD. The broad peaks seen in these diffraction patterns indicate that the crystallite sizes in these carbons are quite small. The peak height decreases with the extent of porosity development, indicating the destruction of the crystalline structures in the etching process. The XRD data reflects that these porous carbons have negligibly small crystallographic domains, and thus the edge sites account for almost all the surface sites for double-layer formation.

The surface characteristics of the carbon-PVDF composites of the electrodes were also determined with N_2 adsorption, and the results are shown in Table III. It can be seen that both the surface

Table II. Surface characteristics of the carbon powders derived from mesophase pitch with KOH etching.

Carbon type	KOH/pitch ratio	Surface area (m^2 g^{-1})	Pore volume (cm^3 g^{-1})	Pore size distribution		Average pore diam (nm)
				micro (%)	meso (%)	
MP131	1.5	1310	0.744	84	16	2.3
MP160	2.0	1600	0.825	93	7	2.1
MP193	2.5	1930	1.00	92	8	2.1
MP196	3.0	1960	1.10	85	15	2.2
MP238	3.5	2380	1.28	88	12	2.2
MP286	4.5	2860	1.63	83	17	2.3

Table III. Surface characteristics of the carbon-PVDF composites of the electrodes.

Carbon type	Surface area (m^2 g^{-1})	Pore volume (cm^3 g^{-1})	Pore size distribution		Average pore diam (nm)
			micro (%)	meso (%)	
MP131	608	0.338	86	14	2.2
MP160	763	0.393	94	6	2.1
MP193	797	0.416	92	8	2.1
MP196	962	0.536	86	14	2.2
MP238	1130	0.594	90	10	2.1
MP286	1370	0.782	83	17	2.3

area and pore volume of the composites are much smaller than those of the carbon powders presented in Table II. Obviously, the PVDF binder has hindered the access of N_2 molecules to the pores in carbon. As for the pore size distribution and average pore diameter, these values are similar for the carbon composites and the powders. This suggests that PVDF has been randomly distributed over the external surface to block some pore entrances. The surface characteristics of the carbon-PVDF composites, rather than the carbon powders, were used as the properties of the electrodes in the following electrochemical investigation.

Electrochemical characteristics of the resulting electrodes.—The typical voltage sweep cyclic voltammograms of the carbon electrodes in 1 M H_2SO_4 are shown in Fig. 2. The voltage sweep range was from -0.9 to 0.9 V and the sweep rates were 2, 5, and 10 mV s^{-1}. The MP286-PVDF composite was employed as the electrodes in the cyclic voltammetric tests. The figure demonstrates that the electrode is stable in the acid solution within the voltage range applied. As the sweep rate increases, it can be observed that there is a widening of the knee of voltammograms just after the reversal of the voltage sweep and an increasing slope of the current plateau. The rectangular form of voltammograms, in which the current quickly reaches a truly horizontal value after the reversal of the voltage sweep, can be observed if the interface forming the double layer is homogeneous and ideally polarizable. Figure 2 exhibits that increasing the sweep rate has enhanced the delay of the current to reach a horizontal value. This is attributable to the enhancement of the distributed capacitance effects in porous electrodes upon increasing the voltage sweep rate.[7] It has been commonly recognized that the charge stored in a porous electrode is distributed,[21-23] and the ohmic resistance in the electrolyte along the axial direction of micropores has the effect of making the mouth of the micropores charge or discharge faster, while the bottom of them lags behind.[22] Under this circumstance, rectangular voltammograms can only be obtained for cyclic voltammetric measurements in which the voltage sweep rates and the corresponding currents are very low, since lowering the current would reduce the potential difference, resulting from the ohmic resistance, between the mouth and the bottom of micropores. An increase in the voltage sweep rate, hence an increase in the potenial difference, would intensify the lag of charge or discharge at the bottom of micropores and thus enhance the delay of the currents to reach a horizontal value in the voltammograms, as shown in Fig. 2.

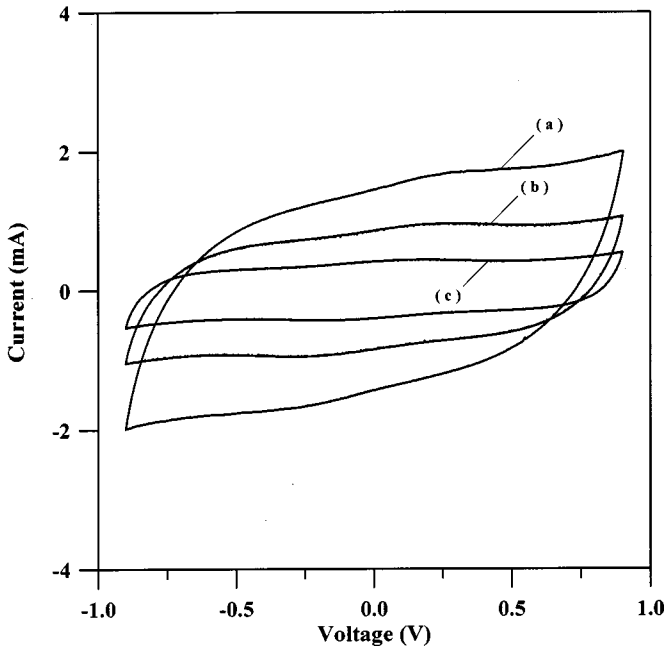

Figure 2. Cyclic voltammograms of MP286 electrode (1 cm^2) in 1 M H_2SO_4 at voltage sweep rates of (a) 10, (b) 5, and (c) 2 mV s^{-1}.

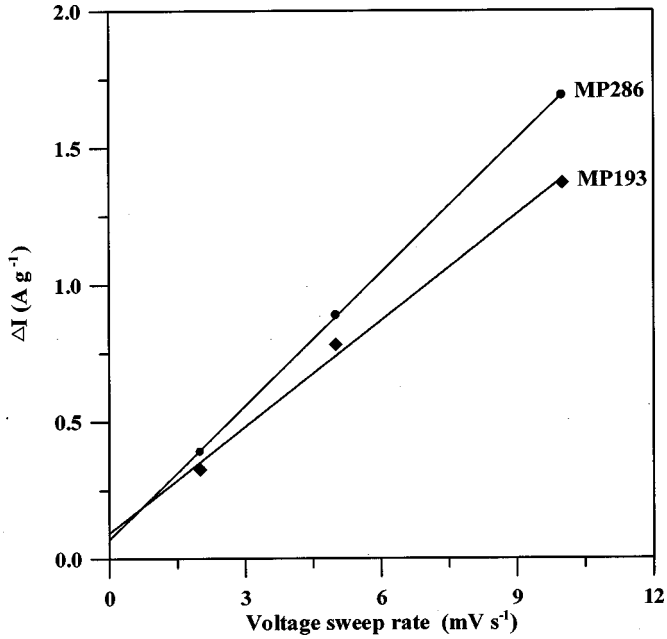

Figure 3. Variation of ΔI (difference between anodic and cathodic charging currents) with voltage sweep rate in cyclic voltammetric measurements using MP193 and MP286 electrodes (1 cm^2).

It can be seen from Fig. 2 that the charging currents for both the anodes and cathodes, I_a and I_c, respectively, are increasing functions of the voltage sweep rate. The difference between I_a and I_c at the current plateaus of the cyclic voltammograms, which was designated as $\Delta I(=I_a - I_c)$, was determined for different voltage sweep rates. The variation of ΔI with the sweep rate for the MP193 and MP286 electrodes is presented in Fig. 3. A linear plot of ΔI against the sweep rate would give the double-layer capacitance and the faradaic current from the slope and intercept of the plot.[24] The calculated results are listed in Table IV. The specific faradaic current (I_F) shows a decreasing trend with the porosity of the carbon electrodes, having a value around 60-80 mA g^{-1}. Why the faradaic

Table IV. Double-layer capacitance and faradaic current of the carbon-PVDF electrodes determined from cyclic voltammograms.

Carbon type	I_F (mA g^{-1})	C_{dl} (F g^{-1})	C'_{dl} (μF cm^{-2})
MP193	75	103	13.0
MP286	57	130	9.4

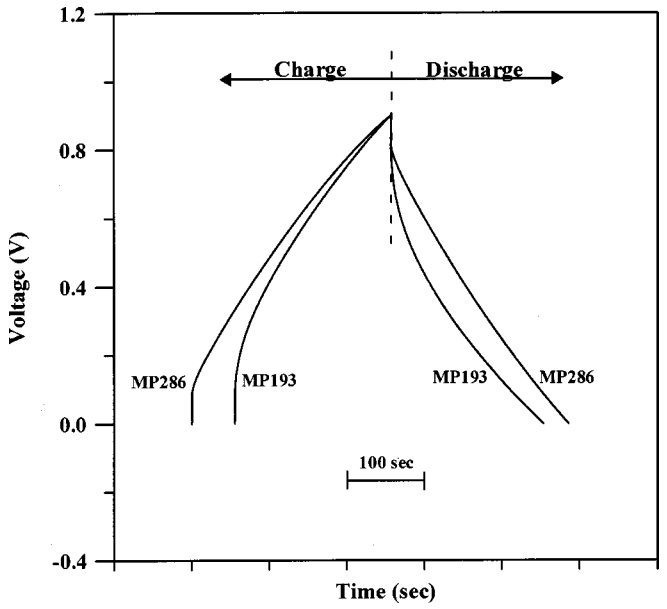

Figure 4. Charge-discharge curves of EDLCs using MP193 and MP286 electrodes (1 cm^2) at 0.5 mA.

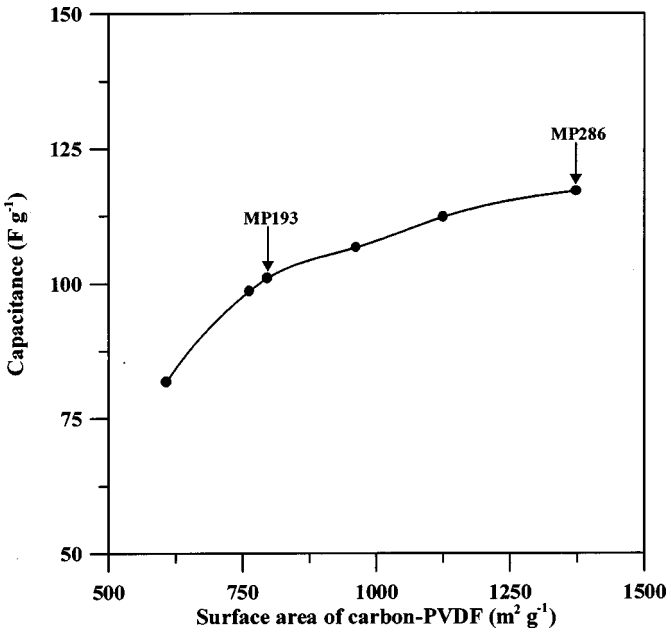

Figure 5. Variation of specific discharge capacitance with specific surface area for electrodes (1 cm^2) charged at 0.5 mA to 0.9 V and then discharged at the same current.

current would vary with the carbon porosity is not clear at this stage of our study. On the other hand, the specific double-layer capacitance (C_{dl}) was found to increase with the porosity of the carbon electrodes. The increase of capacitance was expected, since the carbon surface provides the interface for the formation of the double layers. The double-layer capacitance per unit area of the carbon composites (C'_{dl}) can be calculated, and the results are also provided in Table IV. The value of C'_{dl} was found to be different for different carbon electrodes. Obviously, the applicability of the surface varies with the type of carbon. With more different types of carbon electrodes involved, this aspect is further discussed in the following tests using the charge-discharge cycling.

Performance of capacitors.—Figure 4 shows the typical cell voltage against time curves of EDLCs charged and discharged at a constant current of 0.5 mA. It can be seen that carbon electrodes with a higher porosity have a higher capacitance and better performance in charge and discharge. The specific discharge capacitance of the electrodes (C) in EDLCs can be calculated according to

$$C = (2 \times I \times t)/(W \times \Delta E) \quad [1]$$

where I is the discharge current, t the discharge time, W the carbon composite mass on an electrode, and ΔE the voltage difference in discharge, excluding the portion of IR drop. The factor of two comes from the fact that the total capacitance measured from the test cells is the addition of two equivalent single-electrode capacitors in series. Single-electrode capacitance is reported in the present work.

It has been reported[12] that the electric double-layer capacitance at the electrode surface usually ranges within 10-20 $\mu F\ cm^{-2}$. If the capacitance per unit area has a fixed value for similar porous carbons, the energy stored on the surface should be proportional to the area of the surface. All the carbon electrodes presented in Table III were tested in the same manner shown in Fig. 4, *i.e.*, the electrodes were charged at a constant current of 0.5 mA to a voltage of 0.9 V, and then discharged at a current of 0.5 mA. The specific discharge capacitance of different carbon electrodes were calculated according to Eq. 1, and in Fig. 5 the capacitance results are plotted against the BET surface area of the carbon composites. The data in Fig. 5 show that the values of discharge capacitance for MP193 and MP286 are fairly close to those of C_{dl} (shown in Table IV) determined from the cyclic voltammetric method, although there are some differences that may result from different currents employed for these two methods. Similar to the findings in Table IV, Fig. 5 shows that the specific capacitance increases with the increase in the BET surface area. Apart from the physical structure of such as surface area, the influence of chemical characteristics such as the functionalities of the carbons on the capacitance should also be taken into account. Practically, the chemical properties of carbon are dictated by the type of precursor material used as well as the method of preparation. In the present study, however, these carbons were derived from the same precursor and similar preparation procedures, and the difference exhibited in the pore structure is simply due to the variation in the extent of etching in KOH. Under this circumstance, the influence of chemical characteristics of the carbons on the double-layer formation can be considered to be negligible. The results in both Table IV and Fig. 5 clearly demonstrate that the BET surface area can determine, at least partially, the number of sites available for the formation of double layers.

The influence of the BET surface area can be further explored. If the carbon was constant in character and all the pores were fully and quickly accessible to the double-layer formation on the interface, the specific capacitance would increase proportionally with the increasing surface area. On the other hand, if the pores created during the course of etching were unable to be fully accessed by the electrolyte, which might result from the enhancement of pore resistance to the electrolyte upon etching, then the specific capacitance would not be proportional to the surface area. Under this circumstance, the ratio of specific capacitance to specific BET surface area would decrease with the increasing porosity. This aspect is now examined. Figure 6 shows the ratio of discharge capacitance to BET surface area (capacitance/BET) for carbon composites with different surface areas. It can be seen from the figure that the capacitance/BET ratio shows a significant decrease with the increasing surface area. This result indicates that the quick accessibility to the interface for energy storage was reduced for the new area created upon etching.

Figure 7 shows the variation of micropore and mesopore volumes with the surface area of the carbon composites. It can be seen that the increase in porosity mainly comes from the development of microporosity. The results suggest that the increase in the depth of micropores upon etching might have reduced the accessibility of the surface in micropores to electrolyte, thus leading to the decreased

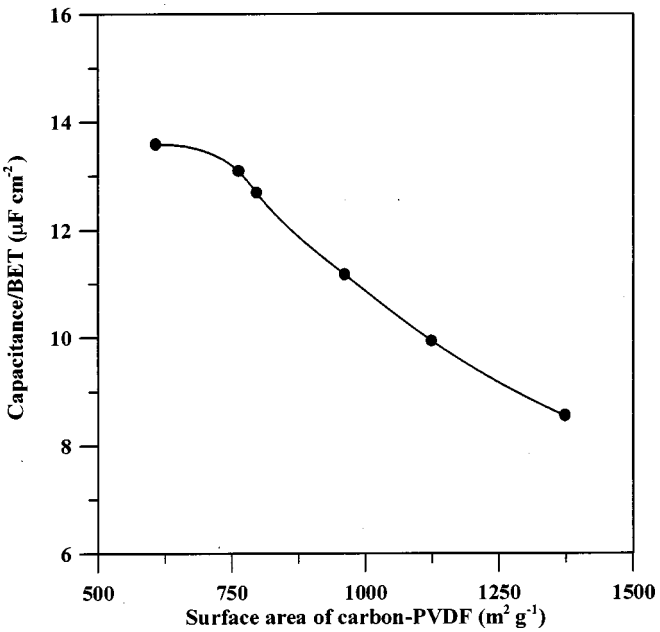

Figure 6. Variation of capacitance/BET ratio with specific surface area for electrodes (1 cm^2) charged at 0.5 mA to 0.9 V and then discharged at the same current.

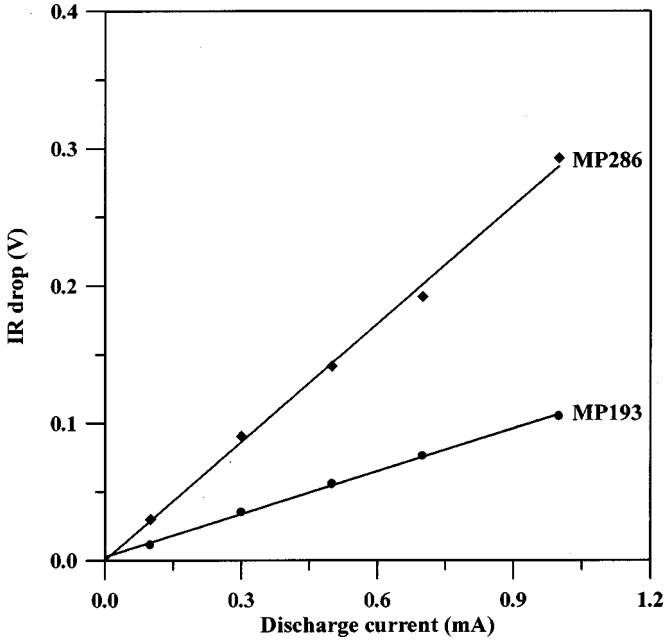

Figure 8. Variation of IR drop with the discharge current for electrodes (1 cm^2) charged at 0.5 mA to 0.9 V.

capacitance/BET ratio with porosity. This also demonstrates that increasing the BET surface area of carbon electrodes does not assure a corresponding linear increase in capacitance.

At the very beginning of the constant current discharge of the EDLCs, the voltage suddenly drops, and this has been designated as the IR drop. This voltage drop can mainly be attributed to the inner resistance of ion diffusion in the micropores of the carbon electrode.[4] Assuming that the diffusion resistance is one of the intrinsic characteristics of the porous carbons, the voltage drop should be proportional to the discharge current. Figure 8 shows the variation of the IR drop with the discharge current for MP193 and MP286 electrodes. It can be seen that the voltage drop increases linearly with the current, and the slope of this linear relationship was used to estimate the resistance of the electrodes. The resistance was found to be 104 and 287 Ω for MP193 and MP286, respectively. This difference in resistance can, at least partially, explain why the capacitance per unit area of MP193 is larger than that of MP286.

Apart from the effect of porosity, the discharge capacitance was found to vary with the discharge current. Figure 9 shows the discharge capacitance of the MP193 and MP286 electrodes charged at a constant current of 0.5 mA to a voltage of 0.9 V and then discharged at different currents. It is observed that the capacitance decreases with discharge current for both electrodes. The decrease of capacitance indicates that the distributed capacitance effects combined with the existence of ohmic resistance along the path of mi-

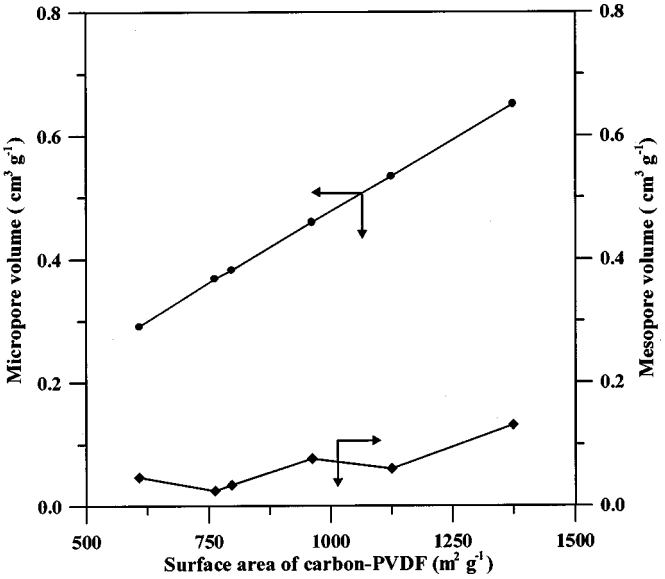

Figure 7. Variation of micropore and mesopore volumes with the surface area of carbon-PVDF composite.

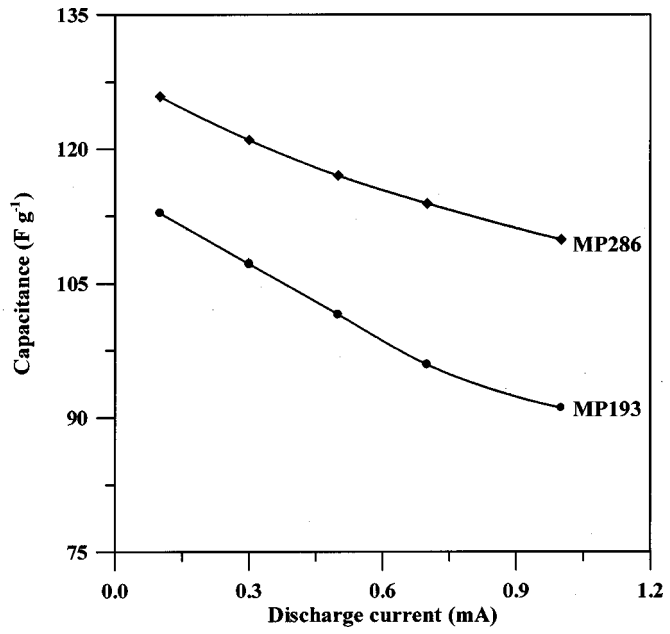

Figure 9. Variation of specific discharge capacitance with the discharge current for electrodes (1 cm^2) charged at 0.5 mA to 0.9 V.

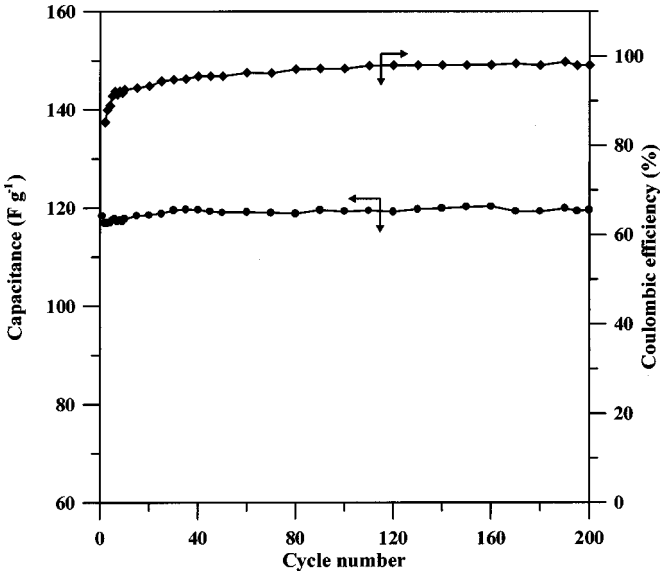

Figure 10. Variation of capacitance stability and coulombic efficiency with cycle number for a MP286 electrode charged and discharged in 1 M H_2SO_4.

cropores has affected the discharge performance of the EDLCs,[21-23] an indication similar to that obtained from the cyclic voltammetric measurements.

To confirm the stability of capacitance and coulomb efficiency with cycling, the EDLC equipped with MP286 electrodes was charged and discharged between 0 and 0.9 V at 0.5 mA. The coulombic efficiency (η) of an EDLC can be calculated from the equation[13]

$$\eta = (t_D/t_C) \times 100$$

where t_D and t_C are the times required for discharging and charging, respectively. The variation of capacitance and coulombic efficiency with cycle number is shown in Fig. 10. The results indicate that the EDLC has stable capacitance (about 120 F g^{-1}) and coulombic efficiency (about 99%) over 200 cycles.

Conclusions

Carbon powders prepared from KOH etching of mesophase pitch were found to have specific surface areas as high as 2860 m^2 g^{-1}. The double-layer capacitance of the carbon-PVDF composites in H_2SO_4 can achieve a value of 130 F g^{-1}. A large proportion of the carbon porosity was found to be obstructed by the PVDF binder, and the surface created by KOH etching cannot be fully utilized as the interface for the formation of double layers. The cyclic voltammetry and the constant current charge-discharge cycling gave fairly close values of the electrode capacitance. The specific capacitance was found to increase with the specific surface area of the carbon composites, but did not show a proportional increase with the surface area. The capacitance per unit carbon-composite area is a decreasing function of the carbon porosity, and this can be attributed to the increase in the micropore depth with the extent of etching. This inference was supported by the observation that resistance determined from the IR drop increases with the porosity. The decrease in capacitance with the discharging current also reflects that the distributed capacitance effects affect the discharge performance. The EDLC prepared in the present work exhibits an excellent cycleability performance with a cycle life of 200 cycles.

Acknowledgments

Financial support from the National Science Council of Taiwan is gratefully acknowledged. The project number is NSC 89-2214-E-006-009. The authors also thank China Steel Chemical Company for supplying the mesophase pitch used in the present work.

National Cheng Kung University assisted in meeting the publication costs of this article.

References

1. L. Bonnefoi, P. Simon, J. F. Fauvarque, C. Sarrazin, and A. Dugast, *J. Power Sources*, **79**, 37 (1999).
2. H. Shi, *Electrochim. Acta*, **41**, 1633 (1996).
3. X. Liu and T. Osaka, *J. Electrochem. Soc.*, **143**, 3982 (1996).
4. X. Liu and T. Osaka, *J. Electrochem. Soc.*, **144**, 3066 (1997).
5. J. M. Miller, B. Dunn, T. D. Tran, and R. W. Pekala, *J. Electrochem. Soc.*, **144**, L309 (1997).
6. R. Saliger, U. Fischer, C. Herta, and J. Fricke, *J. Non-Cryst. Solids*, **225**, 81 (1998).
7. I. Tanahashi, A. Yoshida, and A. Nishino, *J. Electrochem. Soc.*, **137**, 3052 (1990).
8. I. Tanahashi, A. Yoshida, and A. Nishino, *J. Appl. Electrochem.*, **21**, 28 (1991).
9. I. Tanahashi, A. Yoshida, and A. Nishino, *Carbon*, **29**, 1033 (1991).
10. A. Yoshida, S. Nonaka, I. Aoki, and A. Nishino, *J. Power Sources*, **60**, 213 (1996).
11. Y. Kibi, T. Saito, M. Kurata, J. Tabuchi, and A. Ochi, *J. Power Sources*, **60**, 219 (1996).
12. T. Momma, X. Liu, T. Osaka, Y. Ushio, and Y. Sawada, *J. Power Sources*, **60**, 249 (1996).
13. T. Osaka, X. Liu, M. Nojima, and T. Momma, *J. Electrochem. Soc.*, **146**, 1724 (1999).
14. M. J. Munoz-Guillena, M. J. Illán-Gómez, J. M. Martín-Martínez, A. Linares-Solano, and C. Salinas-Martínez de Lecea, *Energy Fuels*, **6**, 9 (1992).
15. J. Laine and S. Yunes, *Carbon*, **30**, 601 (1992).
16. H. Teng and S.-C. Wang, *Carbon*, **38**, 817 (2000).
17. M. J. Illán-Gómez, C. García-García, C. Salinas-Martínez de Lecea, and A. Linares-Solano, *Energy Fuels*, **10**, 1108 (1996).
18. A. Ahmadpour and D. D. Do, *Carbon*, **34**, 471 (1996).
19. T. Wigmans, *Carbon*, **27**, 13 (1989).
20. F. Rodríguez-Reinoso, M. Molina-Sabio, and M. T. González, *Carbon*, **33**, 15 (1995).
21. R. de Levie, *Electrochim. Acta*, **8**, 751 (1963).
22. L. G. Austin and E. G. Gagnon, *J. Electrochem. Soc.*, **120**, 251 (1973).
23. J. R. Miller, in *Electrochemical Capacitors*, F. M. Delnick and M. Tomkiewicz, Editors, PV 95-29, p. 246, The Electrochemical Society Proceedings Series, Pennington, NJ (1996).
24. E. Gileadi, *Electrode Kinetics*, p. 222, VCH Publishers, New York (1993).